

Probing Electron Tunneling Pathways: Electrochemical Study of Rat Heart Cytochrome c and Its Mutant on Pyridine-Terminated SAMs

By: [J. J. Wei](#), Haiying Liu, K. Niki, E. Margoliash and D. H. Waldeck

J. Wei, H.Y. Liu, K. Niki, E. Margoliash, and D. H. Waldeck, "Probing electron transfer pathway of cytochrome c and its mutant immobilized at surface" *Journal of Physical Chemistry B*, **2004**, 108, 16912-16917.

***© American Chemical Society. Reprinted with permission. No further reproduction is authorized without written permission from American Chemical Society. This version of the document is not the version of record. Figures and/or pictures may be missing from this format of the document. ***

This document is the Accepted Manuscript version of a Published Work that appeared in final form in *Journal of Physical Chemistry B*, copyright © American Chemical Society after peer review and technical editing by the publisher. To access the final edited and published work see <https://dx.doi.org/10.1021/jp048148i>

Abstract:

The electron-transfer rates between gold electrodes and adsorbed cytochromes are compared for native cytochrome *c* and its mutant (K13A) using two different immobilization strategies. A recent study by Niki (Niki, K.; Hardy, W. R.; Hill, M. G.; Li, H.; Sprinkle, J. R.; Margoliash, E.; Fujita, K.; Tanimura, R.; Nakamura, N.; Ohno, H.; Richards, J. H.; Gray, H. B. *J. Phys. Chem. B* 2003, 107, 9947) showed that the electron-transfer rate for a particular mutant cytochrome *c* (K13A) is orders of magnitude slower than the native form when electrostatically adsorbed on SAM-coated gold electrodes. The current study directly "links" the protein's heme unit to the SAM, thereby "short circuiting" the electron tunneling pathway. These findings demonstrate that the immobilization strategy can modify the electron-transfer rate by changing the tunneling pathway.

Keywords: cytochrome c | electron tunneling pathway | protein | SAM-coated gold electrodes

Article:

Introduction

The ability to self-assemble chemically well defined monolayer films on electrode surfaces has enabled electrochemical studies of biological molecules and promises to enable the investigation of redox-coupled biological machines. Current applications are limited by the electrical communication between the biological macromolecule and the electrode, however.¹ A number of different strategies have been employed, such as facilitators, redox mediators, direct covalent linkage of the protein or enzyme to the electrode, and protein adsorption. Nevertheless, the control variables for electronic communication through monolayer films have not been clearly delineated. This work describes fundamental studies of the protein cytochrome *c* when it is adsorbed to monolayer-coated electrodes. A comparison of the new results reported here with earlier findings supports the electron tunneling pathway recently identified by Niki et al.² for cytochrome *c*.

A fundamental understanding of electron tunneling in organic and biological molecules has been developed over the past 15 years through a series of well-defined studies in homogeneous solutions. These studies have established that structural features of a molecule play an important role in determining electron tunneling rates. From studies in unimolecular organic supramolecules (composed of a donor unit, an acceptor unit, and a bridging unit), it is clear that the placement and connectivity of atoms determines the magnitude of the electronic coupling between donor and acceptor groups.³ For linear systems, the tunneling probability density flows mostly through the covalent linkages, whereas for systems with a molecular cleft, the preferred tunneling pathway(s) can proceed through noncovalent contacts.⁴ Early work in proteins made either simplified assumptions about the importance of covalent linkages, “the pathway model”,⁵ or totally ignored covalent linkages.⁶ Over time, these two, seemingly divergent, descriptions have evolved and were recently shown to be mathematically isomorphic.^{5a}

With regard to a quantitative understanding of the electron tunneling mechanism, the understanding of heterogeneous electron-transfer reactions lags behind that of intramolecular and intermolecular electron-transfer reactions. Because the transferring electron proceeds from a delocalized state to a localized one (or vice versa) and a continuum of electrode states are available, one might expect the electron tunneling probability at electrodes to differ from that between two localized molecular states. Recent work on simple redox couples has demonstrated that through-bond electron tunneling dominates in some cases⁷ but in other cases tunneling via nonbonded contacts can be dominant.⁸ Niki et al.² have recently studied different mutants of cytochrome *c* that were electrostatically adsorbed to carboxylate surfaces and found an unusual sensitivity for the presence of the protein's lysine-13 amino acid. The current work addresses whether this sensitivity arises from changes in the tunneling pathway for the adsorbed protein or from changes in the energetics of the protein.

Niki, in a recent study, replaces the lysine units on the surface of the cytochrome *c* and studies the electron transfer rate under conditions where the protein is electrostatically adsorbed to the surface. Their work shows that the replacement of lysine-13 with an alanine changes the electron transfer rate by 5 orders of magnitude. When studying a related cytochrome mutant, which swaps the lysine-13 for a glutamic acid (at position 90) that is adjacent on the protein surface, they observed a similar decrease in the rate constant. Because the electrostatic binding should be

similar for this latter mutant and the native system, this result suggests that the adsorption orientation is not solely responsible for the reduced rate constant. Furthermore, they showed that the replacement of lysine-72 or lysine-79 has little effect on the electron transfer rate, even though these are likely binding sites for the cytochrome to the surface.⁹ The proximity of the lysine-13 to the heme is discussed elsewhere.¹⁰ Using the cytochrome *c* crystal structure, one can estimate a physical through-space distance of 5.8 Å from the lysine to the heme and a through-bond distance of about 20 Å. The current work explores this chemically modified system RC9-K13A further to determine whether the reduced rate constant arises from a change in the protein's reorganization energy or is caused by a change in the electron tunneling probability.

The electrochemical rate constant for the RC9-K13A mutant and the native rat cytochrome *c* was measured for two different SAM (self-assembled monolayer)-coated electrodes. In the first case, the electrodes were coated with COOH-terminated SAMs, and in the second case, they were coated with mixed SAMs composed of pyridine and alkane. In the first case, the findings are consistent with the earlier results of Niki et al.² In the second case, however, the mutant and native cytochrome *c* have similar standard electron-transfer rate constants. This finding is consistent with adsorption of the protein to the SAM by axial coordination between the pyridine receptor and the protein's heme;¹¹ both electrochemical^{11a} and spectroscopic^{11b} studies demonstrate that the pyridine receptor binds directly with the heme unit of the protein. In addition, the similarity in the rate constant between the mutant and native form shows that the primary difference between the two cases is the nature of the link between the protein and the electrode.

Experimental Details

Reagents and Materials. Water for the experiments was purified by using a Barnstead-Nanopure system and had a resistivity of 18 MΩ·cm. All mercaptoalkanes were purchased from Aldrich and used without further purification. 4-Mercaptobenzoic acid (97%), 3-mercaptopropionic acid (99%), 6-mercapto-1-hexanol, 11-bromo-1-undecanol (98%), 12-mercapto-1-dodecanol (98+ %), 1-nonadecanol, isonicotinic acid (99%), and docosanedioic acid (85%) were purchased from Aldrich. All pyridine derivatives were synthesized in the manner reported earlier.^{11,12}

Cytochrome *c* (Sigma C 7752, from horse heart, minimum 95% based on a molecular weight of 12 384) was purified using a cation-exchange column (CM-52, carboxymethyl-cellulose from Whatman) in a manner described previously.^{11,12} Rat cytochrome *c* (from rat heart, C7892, 95% based on a molecular weight of 12 132) was purchased from Sigma and used without purification. The preparation of RC9-K13A rat cytochrome *c* mutant was reported elsewhere.¹³ All cytochromes were stored under an argon atmosphere in a freezer until use.

Electrode Preparation. Details of the preparation and characterization of the gold electrode can be found elsewhere.¹¹ A brief outline of the procedure is given here. A gold wire (0.5-mm diameter, 99.99%) was cleaned by reflux in nitric acid (68–70%) at 130 °C for a few hours and then was washed with deionized water. The tip of the gold wire was heated and annealed in a gas flame to form a ball of about 0.06–0.12-cm² surface area.

Chemically modified electrodes were prepared by immersion in an ethanol or THF solution that contained 0.1 mM HS(CH₂)_nOOC(C₅H₄N) and 0.9 mM HS(CH₂)_{n-2}CH₃, where *n* specifies the methylene chain length. The electrode remained in this solution for 1 day to form the mixed SAM. The electrode was removed from the solution, rinsed with absolute ethanol (or THF) and then with the supporting buffer solution (20 mM phosphate buffer pH 7), and finally dried by a stream of argon gas. The electrode was characterized, as previously,¹¹ and then immersed in a solution containing 100 μM cytochrome *c* and 20 mM phosphate buffer (purged with argon gas) for 30 to 60 min. This procedure immobilizes the cytochrome *c* on the SAM-coated electrode.

The electrodes were rinsed with the supporting buffer solution and immersed in a three-electrode electrochemical cell that contained a buffer solution with no cytochrome *c*. Voltammetry was performed on these electrodes.

Electrochemical Measurements. Electrochemical measurements were performed by using an EG&G PAR-283 potentiostat that was controlled by a PC computer running version 4.3 of PARC's 270 software and a GPIB board. The three-electrode cell was composed of a platinum spiral counter electrode, an Ag/AgCl (3 M NaCl) reference electrode, and the SAM-coated Au as a working electrode. The voltammetry measurements were performed in 20 mM phosphate buffer solution (pH of 7.0) under an argon atmosphere. The potentiostat applies a staircase waveform rather than a true analogue signal. For these experiments, the voltage increment was either 1 or 2 mV, and the scan rate ranged from tens of mV/s to 60 V/s. In each case, the current was sampled during the last one-fourth of the potential increment's time window, which is appropriate for a relatively high scan rate and proper kinetic analysis.

The uncompensated resistance (R_u) in the 20 mM buffer solution during the voltammetry measurements can sometimes be important for the data analysis at high scan rates. The measured R_u in these studies ranges from 200 to 500 Ω depending on the distance between electrodes, the geometry, and the electrode areas. The calibrated peak potential in this work was corrected by the following equation

$$E_c(t) = E_a(t) - i(t)R_u$$

where $E_c(t)$ is the calibrated potential, $E_a(t)$ is the applied (apparent) potential, and $i(t)$ is the current of the voltammogram. An average resistance of $R_u = 300 \Omega$ was used. Because of the low currents in this study, the electron-transfer rate constants obtained both from the apparent and corrected peak potentials differ little.

For an electron-transfer rate constant measurement by cyclic voltammetry, the method is limited in its time resolution by the *rc* characteristics of the electrode. With the small-diameter (ca. 1 mm) gold ball electrodes used in this work, rate constants can be measured up to 10 000 s⁻¹.

Results

The protein was adsorbed on the surface in two different ways (Figure 1). The case 1 method adsorbed the protein electrostatically to electrodes that were coated with a monolayer-thick film of carboxyl-terminated alkanethiols. This method is well established.¹⁴ The case 2 method

adsorbed the protein onto mixed monolayer films composed of pyridine-terminated alkanethiols and alkanethiols. Previous work presents ac impedance, electrochemistry, and STM studies of the case 2 SAMs and the adsorbed protein.¹¹ In both cases, the solution has a pH of 7 with 20 mM phosphate buffer.

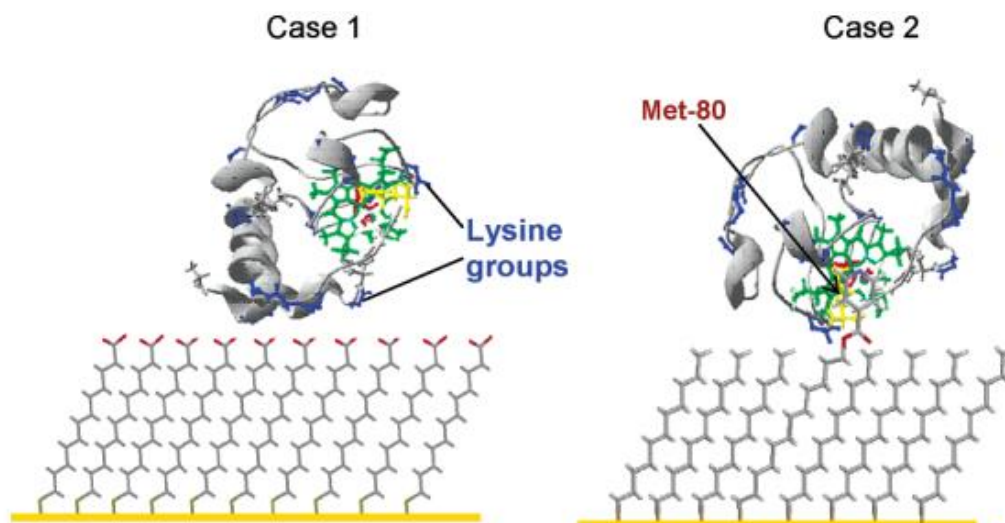


Figure 1. Cytochrome *c* adsorption on self-assembled monolayers. Case 1: electrostatic adsorption on carboxylic acid SAM. Case 2: Ligand-immobilized cytochrome *c* on pyridine-terminated mixed SAM.

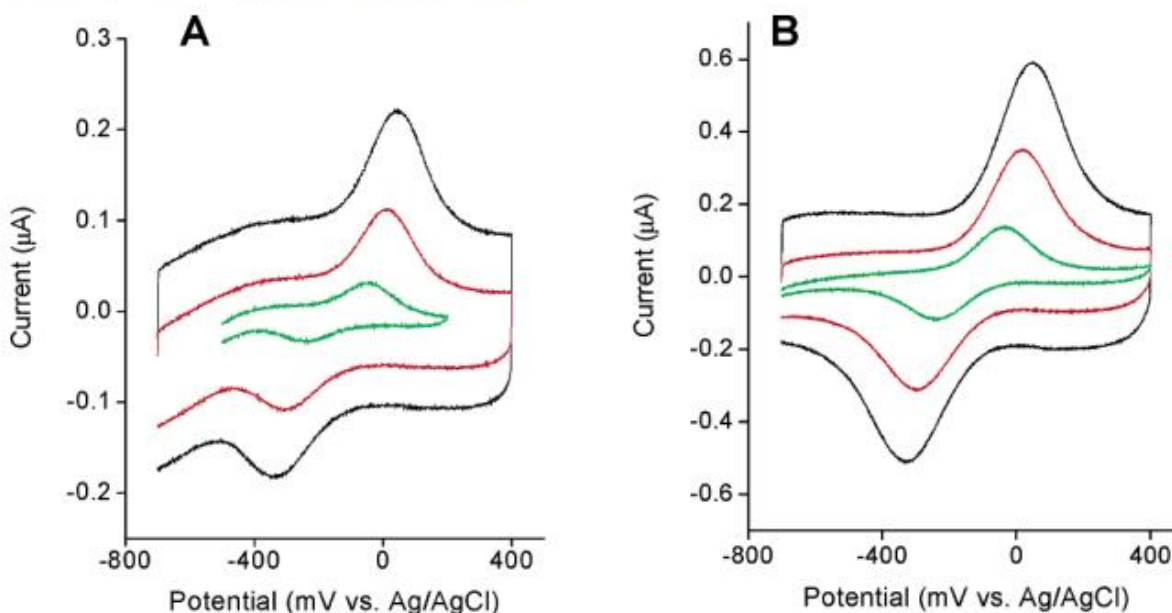


Figure 2. Representative cyclic voltammograms of native rat cytochrome *c* and rat mutant K13A immobilized on C20Py/C19 mixed monolayer modified gold electrodes. (A) Native cytochrome *c*. (B) Rat mutant K13A. Scan rates are 0.2 V/s (green), 0.6 V/s (red), and 1.0 V/s (black).

Cyclic Voltammetry and Electron-Transfer Rate Constant. Rat heart cytochrome *c* and mutant K13A were immobilized on gold electrodes that were modified using the pyridine receptors. The adsorbed cytochrome *c*'s redox response was studied by using cyclic voltammetry over the potential range from -0.8 to 0.4 V. A signature for the immobilization of the protein by the pyridine is a negative shift of its redox potential. (For horse heart cytochrome *c*, it shifts to -0.172 V versus Ag/AgCl.) This value is indicative of the replacement of the heme's axial

methionine ligand with the pyridine under conditions that do not unfold the entire redox center.^{10,11}

Figure 2 shows representative cyclic voltammograms of native rat heart cytochrome *c* (panel A) and the mutant (panel B) immobilized on a gold electrode with C20OOC-Py/C19 alkanethiol mixed SAMs. The data present well-defined peaks with a formal potential at -0.147 ± 0.006 V for native cytochrome *c* and at -0.146 ± 0.011 V for the mutant cytochrome *c*. These data also show the increase in peak separation with the increase in voltage scan rate. The Supporting Information shows the linear relationship between the peak current (I_p) and scan rate (v). This latter dependence confirms that the protein is adsorbed on the electrode surface rather than diffusing in solution.

The rate constant was determined by fitting the peak potential shift as a function of the scan rate to the classical Marcus theory in the manner described previously.^{11,15} In this analysis, a reorganization energy of 0.58 eV was applied to obtain the standard electron-transfer rate constant (vide infra) under the assumption that the reaction's symmetry factor is 0.5. Simulations of the cyclic voltammograms indicate that symmetry factors of 0.46 for mutant K13A and 0.41 for native rat cytochrome *c* are more appropriate; however, the comparisons between data sets is facilitated by approximating the symmetry factor with the value 0.5. This choice does not affect the reported rate constants very strongly. For example, the mutant's anodic electron-transfer rate constant is 0.63 s^{-1} , and its cathodic electron-transfer rate constant is 0.60 s^{-1} when using a symmetry factor of 0.46. These rate constants are very close to the 0.62-s^{-1} value obtained from the factor 0.5.

The standard heterogeneous rate constants k_{et}^0 for the different systems of the native cytochrome *c* and mutant are summarized in Table 1. These data are in good agreement with the findings of earlier work.^{2,10,18}

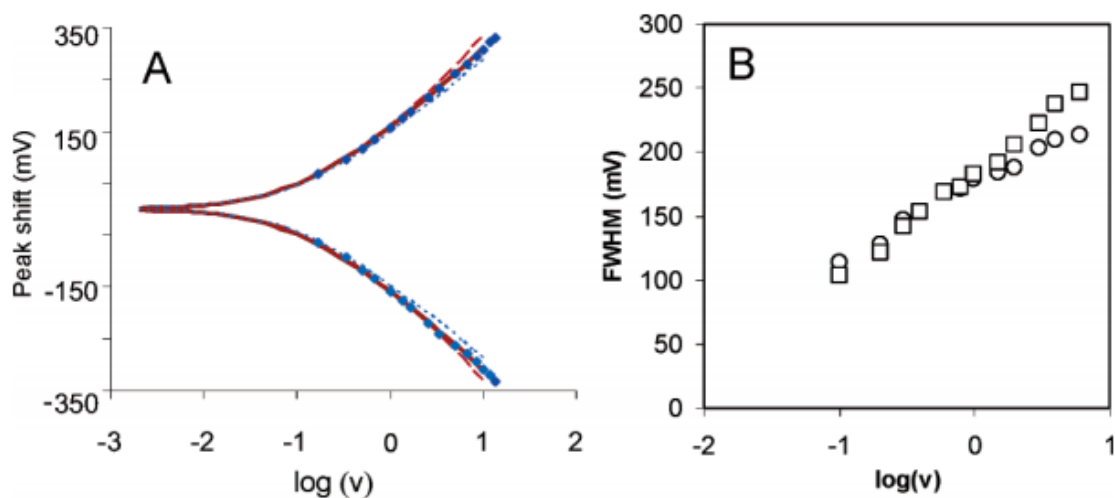


Figure 3. (A) Experimental peak shift for native rat cytochrome *c* plotted vs $\log(v)$, where v is the voltage scan rate. The three curves are calculated from the Marcus model at reorganization energies of (a) 0.30 eV, red dashed curve; (b) 0.58 eV, solid curve; and (c) 0.90 eV, dotted curve. The best fit is at $k_{\text{et}}^0 = 0.62 \text{ s}^{-1}$ and reorganization $\lambda = 0.58 \text{ eV}$. (B) Increase in the fwhm for the voltammogram as a function of the scan rate (\square , reduction wave; \circ , oxidation wave).

TABLE 1: Electron-Transfer Rate Constant of Rat Heart Cytochrome *c* and the Mutant K13A Adsorbed on Different Electrodes^a

systems	native cytochrome <i>c</i>		mutant K13A	
	k_{et}^0	no. of trials	k_{et}^0	no. of trials
C6Py/C5			789 ± 155	3
C11Py/C10	903 ± 130	3	816 ± 122	4
C12Py/C11	770 ± 42	3	737 ± 103	3
C16Py/C15	55.3 ± 2.1	3	80 ± 16	5
C20Py/C19	0.62 ± 0.03	3	0.73 ± 0.12	4
C3COOH	920 ± 60	2	0.13 ± 0.04	2
(C ₆ H ₄)COOH	570 ± 45	5	0.20 ± 0.06	2
C5COOH	680 ± 68	5	0.0035 ± 0.001	4
C10COOH	19 ± 7.2	4		

^a Errors indicated for the rate constant represent one standard deviation from the average value found for the different trials.

Reorganization-Energy Measurement. In principle, the reorganization energy of cytochrome *c* and the mutant can be obtained by fitting the peak shift with voltage scan rate to the Marcus model. In practice, one must access high voltage scan rates so that significant overvoltage is probed.¹⁶ By studying thick films, thereby slowing the electron-transfer rate, and accessing higher scan rates, the reorganization energy for the pyridine-immobilized protein was probed. Figure 3A shows data for the peak shift versus the voltage scan rate of the native rat cytochrome *c* immobilized on a C20Py/C19 mixed film. At slow enough scan rates, the peak separation should go to zero. Because of the signal-to-noise ratio, this limit was not reached for the C20Py films; however, very small peak separations were found for the shorter alkanethiols (e.g., 5 mV for C12Py/C11; see ref 18 and Supporting Information). Figure 3B shows how the voltammogram width changes with scan rate. At slow scan rates, where the voltammogram is reversible, the width should be 91 mV, and it increases as the scan rate makes the electron-transfer process more irreversible. Note that high scan rates show that the reduction wave is broadened, as compared to the oxidation wave. This feature may reflect the importance of conformational changes at higher scan rates.^{11b}

Three different fits, corresponding to λ values of 0.3, 0.58, and 0.9 eV, of the Marcus model to the data in Figure 3A are shown. The best fit occurs for $\lambda = 0.58$ eV and a standard electron-transfer rate constant of $k^0 = 0.62$ s⁻¹. By using this analysis, the reorganization energy of both native rat cytochrome *c* and mutant K13A cytochrome *c* can be determined. These results are summarized in Table 2. Average reorganization energies of 0.6 eV for mutant K13A and 0.6 eV for native cytochrome *c* are obtained. These reorganization energies are similar to those reported for native cytochrome *c* in solution.¹⁷ The error in determining the reorganization energy is between 0.1 and 0.2 eV; see Supporting Information for quantitative details.

TABLE 2: Summary of Reorganization Energy Measurements of Rat Heart Cytochrome *c* and Mutant K13A Obtained from Immobilization on C20Py/C19 Mixed Monolayer Films

trial	mutant K13A cytochrome <i>c</i>			native cytochrome <i>c</i>		
	k^0 (s^{-1})	λ (eV)	E^0 (mV)	k^0 (s^{-1})	λ (eV)	E^0 (mV)
1	0.82	0.50	-150	0.60	0.62	-141
2	0.85	0.45	-157	0.65	0.55	-153
3	0.66	0.70	-132	0.62	0.58	-148
4	0.60	0.65	-145			
av	0.7 ± 0.1	0.6 ± 0.1^a	-146 ± 11	0.62 ± 0.03	0.58 ± 0.04^a	-147 ± 6

^a The error in the λ determination is larger than the dispersion found in these trials. See Supporting Information for details.

Distance Dependence of Electron Transfer. The protein's electron-transfer rate constant was measured as a function of distance from the electrode surface. The distance between the protein and the electrode was systematically varied by changing the thickness of the SAM. Figure 4 presents the distance dependence of the measured electron-transfer rate constant of rat heart cytochrome *c* and the K13A mutant immobilized on pyridine systems. The data are similar to the results obtained earlier for horse heart cytochrome *c* (also shown).^{11,18} Data are also shown for the proteins adsorbed on carboxylate-terminated monolayers.²

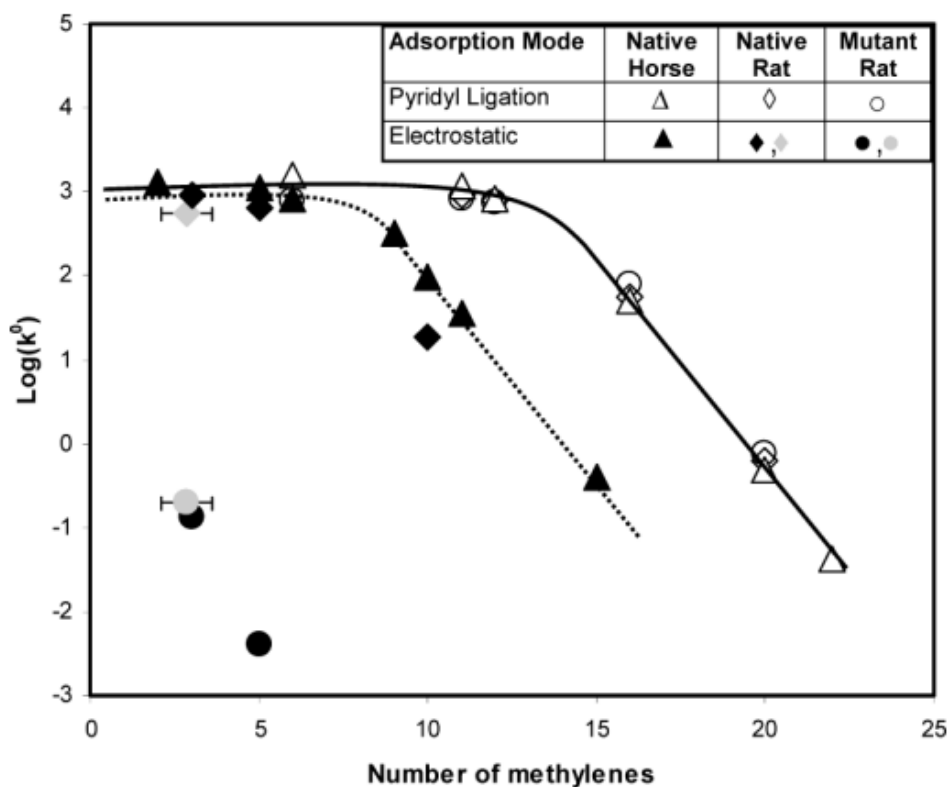


Figure 4. Measured electron-transfer rate constant of surface-immobilized rat heart cytochrome *c* and its K13A mutant plotted as a function of SAM thickness. The solid curve and the dashed curve represent the distance dependence of native horse heart cytochrome *c* with the pyridine and carboxylic acid system, respectively. The gray symbols are for a $S(C_6H_4)COOH$ monolayer, and the bar shows the uncertainty in assigning it a length equivalent to some number of methylenes.

For the pyridine-terminated films (open symbols), the native rat cytochrome *c* and the K13A cytochrome *c* rate constants are within 15% of each other, and they show a qualitatively similar dependence on the SAM thickness. The data display a plateau region at short donor–acceptor separations, which demonstrates that the two proteins have similar rate constants in this solvent-controlled regime.^{10,18} At large separations, the electron-transfer rate constant displays an

exponential dependence on the charge-transfer distance with decay coefficients of 1.12 per methylene for the native cytochrome and 1.16 per methylene for the mutant (dashed line). This distance dependence is similar to that found in other tunneling studies with saturated hydrocarbons and is a signature of nonadiabatic electron transfer. For a more detailed discussion and analysis of the electron transfer in these two regimes, (plateau region and tunneling region) see refs 10 and 18.

In contrast to the SAMs with pyridine receptors, the carboxyl-terminated monolayers display different rate constants for the native and mutant forms of cytochrome *c*. At low film thickness, the native cytochrome *c* approaches the limiting (plateau) value¹⁹ observed for the pyridine-tethered protein. In contrast, the mutant cytochrome *c* never reaches this value, and its rate constant is consistently lower (by orders of magnitude) than that of the native cytochrome. Although the data for the mutant form appears to fall off exponentially with distance, no fit is shown through the data because of the few number of points.²⁰ This observation agrees with the findings reported earlier.²

Discussion

The data clearly show that the method of binding cytochrome *c* to the monolayer film can be used to modify the electron-transfer rate constant by changing the electron-tunneling pathway. For the electrostatic binding mode (case 1), the electron-transfer rate constant of the native cytochrome *c* differs by 5 orders of magnitude from that found for the K13A mutant. In this protein assembly, the outer surface of the protein contacts the outer surface of the SAM so that electrons must tunnel through a portion of the protein's peptide chain to reach the redox center. In contrast, the immobilization of cytochrome *c* by direct linkage of the protein's heme unit with the SAM's pyridine receptor has similar rate constants for the mutant and the native protein. This similarity results because the electron-tunneling pathway along the alkane tether of the pyridinal receptor is the same in these two cases. Furthermore, the dependence of this electron-transfer rate constant on the length of the alkane tether is qualitatively similar to that found for horse heart cytochrome *c*, even though the apparent redox potentials differ by 25 mV.

The reorganization energy of the cytochrome *c* could be determined for the slower electron-transfer rate constants. In these cases, the reorganization energy was found to be about 0.6 eV and to vary little between the mutant and native forms or the method of immobilization. In fact, this value of the reorganization energy is similar to that reported for cytochrome *c* in free solution.¹⁷ The similarity of the reorganization energies for the mutant and native forms, when pyridine ligated, suggests that the mutation has little impact on the reorganization energy. Surprisingly, the pyridine-ligated native form has a reorganization energy similar to that found for the native form when not ligated, implying that the pyridine ligation does not strongly modify or control the reorganization energy. This observation is consistent with other studies that conclude that the reorganization energy in cytochrome *c* is primarily “outer sphere” and arises from small contributions of many different protein and solvent modes.²¹ Although the error in the reorganization energy could be as high as 0.2 eV, such a difference would change the standard rate constant by less than 1 order of magnitude, as compared to the 4 to 5 orders of magnitude difference between the two immobilizations of the mutant protein. These findings

argue against an energy effect causing the dramatic decrease in the rate constant for lysine-13 when it is adsorbed onto carboxylate films.

These studies support the conclusion that the reduced electron-transfer rate constant for the K13A mutant adsorbed on carboxylate films results from the blocking of an efficient electron-tunneling pathway. When adsorbed onto carboxylate films, the electron must tunnel through the protein to reach the heme. When adsorbed through the pyridine receptors, the electron tunnels through the artificial tether and is not impacted by changes in the native protein's electron-transfer pathways.

Acknowledgment

We thank the U.S.–Israel Binational Science Foundation for partial support of this work.

Supporting Information Available

Assessment of the errors associated with the rate constant and reorganization energy determination, full width at half height and peak shifts for the mutant voltammogram as a function of scan speed, fwhm data for different monolayer films, and the dependence of the current on scan speed. This material is available free of charge via the Internet at <http://pubs.acs.org>.

References and Notes

- (1) (a) Willner, I.; Katz E. *Angew. Chem., Int. Ed.* **2000**, *39*, 1180. (b) Willner, I.; Willner, B. *Trends Biotechnol.* **2001**, *19*, 222.
- (2) Niki, K.; Hardy, W. R.; Hill, M. G.; Li, H.; Sprinkle, J. R.; Margoliash, E.; Fujita, K.; Tanimura, R.; Nakamura, N.; Ohno, H.; Richards, J. H.; Gray, H. B. *J. Phys. Chem. B* **2003**, *107*, 9947.
- (3) (a) Oevering, H.; Paddon-Row: M. N.; Heppener, M.; Oliver, A. M.; Costaris, E.; Verhoeven, J. W.; Hush, N. S. *J. Am. Chem. Soc.* **1987**, *109*, 3258. (b) Closs, G. L.; Calcaterra, L. T.; Green, N. J.; Penfield, K. W.; Miller, J. R. *J. Phys. Chem.* **1986**, *90*, 3673. (c) Helms, A.; Heiler, D.; McLendon, G. *J. Am. Chem. Soc.* **1992**, *114*, 6227. (d) Helms, A.; Heiler, D.; McClendon G. *J. Am. Chem. Soc.* **1991**, *113*, 4325. (e) Sakata, Y.; Tsue, H.; O'Neil, M. P.; Wiederrecht, G. P.; Wasielewski, M. R. *J. Am. Chem. Soc.* **1994**, *116*, 6904. (f) Penfield, K. W.; Miller, J. R.; Paddon-Row: M. N.; Cotsaris, E.; Oliver, A. M.; Hush, N. S. *J. Am. Chem. Soc.* **1987**, *109*, 5063. (g) Pispisa, B.; Venanzi, M.; Palleschi, A. *J. Chem. Soc., Faraday Trans.* **1994**, *90*, 435. (h) Finckh, P.; Heitele, H.; Volk, M.; Michel-Beyerle, M. E. *J. Phys. Chem.* **1988**, *92*, 6584. (i) Wasielewski, M. R.; Niemczyk, M. P.; Johnson, D. G.; Svec, W. A.; Minsek, D. W. *Tetrahedron* **1989**, *45*, 4785. (j) Zehnacker, A.; Lahmani, F.; Van Walree, C. A.; Jenneskens, L. W. *J. Phys. Chem. A* **2000**, *104*, 1377.
- (4) Waldeck, D. H.; Zimmt, M. B. *J. Phys. Chem. B* **2003**, *107* 3580.

- (5) (a) Jones, M. L.; Kurnikov, I. V.; Beratan, D. N. *J. Phys. Chem. A* **2002**, *106*, 2002 and references therein. (b) Gray, H. B.; Winkler, J. R. *Annu. Rev. Biochem.* **1996**, *65*, 537.
- (6) Moser, C. C.; Keske, J. M.; Warncke, K.; Farid, R. S.; Dutton, P. L. *Nature* **1992**, *355*, 796.
- (7) Napper, A. M.; Liu, H.; Waldeck, D. H. *J. Phys. Chem. B* **2001**, *105*, 7699.
- (8) Yamamoto, H.; Waldeck, D. H. *J. Phys. Chem. B* **2002**, *106*, 7469.
- (9) These observations are consistent with the reduced enzyme activity of cytochrome *c* oxidase in the presence of the lysine-13 modified protein. See (a) Theodorakis, J. L.; Garber, E. A. E.; McCracken, J.; Peisach, J.; Schejter, A.; Margoliash, E. *Biochim. Biophys. Acta* **1995**, *1252*, 103–113. (b) Theodorakis, J. L.; Armes, L. G.; Margoliash, E. *Biochim. Biophys. Acta* **1995**, *1252*, 114. (c) Smith, H. T.; Ahmed, A. J.; Millett, F. J. *Biol. Chem.* **1981**, *256*, 4984 (for a diagram of the binding).
- (10) Khoshtariya, D. E.; Wei, J.; Liu, Haiying; Yue, H. J.; Waldeck, D. H. *J. Am. Chem. Soc.* **2003**, *125*, 7704.
- (11) The primary evidence for the direct ligation between the pyridine and the heme unit is the negative shift in redox potential and the Raman spectra for the adsorbed protein. See (a) Wei, J.; Liu, H.; Dick, A.; Yamamoto, H.; He, Y.; Waldeck, D. H. *J. Am. Chem. Soc.* **2002**, *124*, 9591. (b) Murgida, D. H.; Hildebrandt, P.; Wei, J.; He, Y.-F.; Liu, H.; Waldeck, D. H. *J. Phys. Chem. B* **2004**, *108*, 2261.
- (12) Yamamoto, H.; Liu, H.-Y.; Waldeck, D. H. *Chem. Commun.* **2001**, 1032.
- (13) Niki, K.; Pressler, K. R.; Sprinkle, J. R.; Li, H.; Margoliash, E. *Russ. J. Electrochem.* **2002**, *38*, 74–78.
- (14) (a) Song, S.; Clark, R. A.; Bowden, E. F.; Tarlov, M. J. *J. Phys. Chem.* **1993**, *97*, 6364. (b) Avila, A.; Gregory, B. W.; Niki, K.; Cotton, T. M. *J. Phys. Chem. B* **2000**, *104*, 2759.
- (15) Napper, A. M.; Liu, H.; Waldeck, D. H. *J. Phys. Chem. B* **2001**, *105*, 7699.
- (16) (a) Finklea, H. O. In *Electroanalytical Chemistry*; Bard, A. J., Rubinstein, I., Eds.; Marcel Dekker: New York, 1996; Vol. 19, p 109. (b) Chidsey, C. E. D. *Science* **1991**, *251*, 919. (c) Miller, C. J. In *Physical Methods in Electrochemistry*; Rubinstein, I., Ed.; Wiley: New York, 1995; p 27.
- (17) (a) Terrettaz, S.; Cheung, J.; Miller, C. J. *J. Am. Chem. Soc.* **1996**, *118*, 7857. (b) Winkler, J. R.; DiBilio, A. J.; Farrow, N. A.; Richards, J. H.; Gray, H. B. *Pure Appl. Chem.* **1999**, *71*, 1753.
- (18) Wei, J.; Liu, H.-Y., Khoshtariya, D. E.; Yamamoto, H.; Dick, A.; Waldeck, D. H. *Angew. Chem.* **2002**, *41*, 4700.
- (19) Feng, Z. Q.; Imabayashi, S.; Kakuichi, T.; Niki, K. *J. Chem. Soc., Faraday Trans.* **1997**, *93*, 1367.

(20) Attempts to adsorb the protein onto thinner films gave a faradaic response, but the apparent redox potential of the protein was shifted considerably from the other data. Because those results are suspect, they are not included. Attempts to study thicker films were not fruitful because the signal is too weak.

(21) (a) Sigfridsson, E.; Olsson, M. H. M.; Ryde, U. *J. Phys. Chem. B* **2001**, *105*, 5546. (b) Muegge, I.; Qi, P. X.; Wand, A. J.; Chu, Z. T.; Warshel, A. *J. Phys. Chem. B* **1997**, *101*, 825. (c) Lewgrand, N.; Boudon, A.; Simmonneaux, G. *Inorg. Chem.* **1996**, *35*, 1627. (d) Basu, G., Kitao, A.; Kuki, A.; Go, N. *J. Phys Chem. B* **1998**, *102*, 2085.